

ELECTRIC MONOPOLE TRANSITIONS AND STRUCTURE OF  $^{150}\text{Sm}$ 

SOHAIR M. DIAB

Faculty of Education, Phys. Dept., Ain Shams University, Cairo, Roxy, Egypt

*Received May 16, 2007*

The contour plot of the potential energy surfaces  $V(\beta, \gamma)$  shows that  $^{150}\text{Sm}$  is a spherical nucleus and has vibrational characters. The vibrational limit of the interacting boson approximation model (IBA-2) has been applied. Levels belonging to the ground state (g.s), beta ( $\beta$ ) and gamma ( $\gamma$ ) bands are successfully reproduced. The transition probabilities of gamma transitions are calculated as well as the strength  $X_{if}(E0/E2)$  of electric monopole, ( $E0$ ), transitions. The calculated values are compared with the available experimental and theoretical data. A reasonable agreement has obtained between both.

## INTRODUCTION

The phase transition from spherical to deformed shape which takes place in Sm isotopes has stimulated many authors to study theoretically and experimentally the area of these isotopes. The transition occurs between  $^{150}\text{Sm}$  and  $^{152}\text{Sm}$ . The former is a vibrational-like isotope while the latter is a rotational-like one.

The cross section for proton scattering to the ground state has been studied [1] and the low-lying collective states of even stable samarium isotopes were measured at an incident energy of 25.6 MeV. The results are analyzed in terms of the strong coupling approximation assuming the  $^{144-150}\text{Sm}$  nuclei to be harmonic vibrator.

The elastic and inelastic scattering of  $^{16}\text{O}$  on  $^{148,150,152}\text{Sm}$  isotopes were studied [2] and led to the first  $2^+$  state for the three isotopes. The  $4^+$  state for  $^{152}\text{Sm}$  has been measured at several energies in the vicinity of Coulomb barrier.

The cross section of helion scattering leading to the ground state and the first four to six excited states of the even-even stable samarium isotopes were measured at incident energy of 40.9 MeV [3]. The results are analyzed in terms of the strong coupling approximation assuming the  $^{144,148}\text{Sm}$ ,  $^{150}\text{Sm}$  and  $^{152,154}\text{Sm}$  nuclei to be harmonic vibrators, an asymmetric rotor and symmetric rotors respectively. A systematic study was carried out to deduce the  $2\gamma$  ( $\gamma = 2, 3, 4, 6$ ) pole deformation parameters and a single common optical model

potential for this nuclear range. A description of the elastic and inelastic scattering cross section is given in the framework of the coupled-channels theory and the collective model.

The spectra, quadrupole transition rates, and quadrupole moments of the even-even samarium isotopes were calculated in a schematic model [4] which truncates the valence nucleon states to those which have pairs of protons and pairs of neutrons coupled coherently to angular momentum zero and angular momentum two only. However no boson approximation is made. The hamiltonian consists mainly of pairing between identical nucleons, and a quadrupole-quadrupole interaction between neutrons and protons with coupling strengths independent of atomic mass.

The interacting boson model (IBA) has been used [5] to interpret the ground state charge distributions and lowest  $2^+$  transition charge densities of the even samarium isotopes  $A = 144-154$ . Also, [6] has used the effective IBA hamiltonian to describe the low-lying energy spectra of several series of even-even isotopes. Applications are made to the Xe, Ba, Sm, Gd and U isotopes. In each case a single effective IBA hamiltonian containing at most six parameters reproduces some 50 experimental energies with an rms deviation of about 100 keV or less.

The boson expansion theory was applied [7] to Ru, Pd, Sm, Os and Pt isotopes. The energies, quadrupole moments and transition probabilities of low-lying collective states were calculated.

In the present work the vibrational limit of the IBA-2 has been applied to  $^{150}\text{Sm}$ . The levels energy, transition probabilities  $B(E2)$ 's, electric monopole strength  $X_{iff}(E0/E2)$  and the potential energy surfaces of the nucleus has been calculated and compared with the available experimental data.

## 2. FORMALISM

### 2.1. LEVEL ENERGIES

The IBA-2 model [8–10] was applied to the positive-parity of the low-lying states in  $^{150}\text{Sm}$ . The hamiltonian employed for the present calculation [11] is:

$$H = \varepsilon_{\pi}(d^+ \times d)_{\pi} + \varepsilon_{\nu}(d^+ \times d)_{\nu} + V_{\pi\pi} + V_{\nu\nu} + KQ_{\pi} \cdot Q_{\nu} + M_{\pi\nu} \quad (1)$$

where  $\varepsilon_{\pi}$ ,  $\varepsilon_{\nu}$  are the  $\pi$  and  $\nu$  energies respectively and they are assumed equal

$$\varepsilon_{\nu} = \varepsilon_{\pi} = \varepsilon$$

The third and fourth term of eq. (1) represent the proton-neutron interactions operator which is given by

$$V_{\rho\rho} = \sum_{L=0,2,4} \frac{1}{2} C_{L\rho} (2L+1)^{\frac{1}{2}} \left[ (d^+ \times d^+)_\rho^L \cdot (d \times d)_\rho^L \right]^{(0)} \quad \rho = \pi \text{ or } \nu \quad (2)$$

The fifth term is the quadrupole operator which is given by the usual expression ( $K$  is the strength of the proton and neutron bosons quadrupole interactions)

$$Q_\rho = \left[ (s^+ \times d) + (d^+ \times s) \right]_\rho + x_\rho (d^+ \times d)_\rho \quad \rho = \pi \text{ or } \nu \quad (3)$$

The sixth term is the Majorana operator and is given by

$$M_{\pi\nu} = -2 \sum_{k=1,3} \varepsilon_k (d_\pi^+ \times d_\nu^+)^k \cdot (d_\pi \times d_\nu) + \varepsilon_2 (d_\pi^+ \times s_\nu^+ - s_\pi^+ \times d_\nu^+)^{(2)} \cdot (d_\pi \times s_\nu - s_\pi \times d_\nu) \quad (4)$$

## 2.2. REDUCED TRANSITION PROBABILITIES, $B(E2)$ 's

The electric quadrupole transition operator [8] employed in this study is:

$$T^{(E2)} = e_\pi Q_\pi + e_\nu Q_\nu \quad (5)$$

where:

$T^{(E2)}$ : absolute transition probability of the electric quadrupole ( $E2$ ) transition,

$e_\pi$  and  $e_\nu$ : the proton ( $\pi$ ) and neutron ( $\nu$ ) effective charges respectively, and

$Q_\rho$ : the quadrupole operators which are the same as that in eq. (3)  $\rho = \pi$  or  $\nu$ .

The reduced electric quadrupole transition rates between  $I_i \rightarrow I_f$  states are given by

$$B(E2, I_i \rightarrow I_f) = \left[ \langle I_f \| T^{(E2)} \| I_i \rangle \right]^2 / (2I_i + 1) \quad (6)$$

where

$I_i$ : the initial state of the electric quadrupole transition, and

$I_f$ : the final state of the electric quadrupole transition.

The  $\pi$  and  $\nu$  boson numbers  $N_\pi$  and  $N_\nu$  respectively can be treated as parameters. They are fixed to be half the number of valence fermions and counted from the nearest closed shell.

The effective charges  $e_\pi$  and  $e_\nu$  depend on the total number of bosons  $N$ , number of  $\nu$  bosons  $N_\nu$ , number of  $\pi$  bosons  $N_\pi$  and the experimental value of  $B(E2, 2_1^+ \rightarrow 0_1^+)$ , where

$$N = N_\pi + N_\nu \quad (7)$$

The effective charges of the vibrational limit are calculated using [12]:

$$(N_\pi)^{-1}[(N)(N+3)^{-1}B(E2, 2_1^+ \rightarrow 0_1^+)]^{1/2} = e_\pi + e_\nu N_\nu / N_\pi \quad (8)$$

### 3. CALCULATIONS, RESULTS AND DISCUSSION

#### 3.1. THE POTENTIAL ENERGY SURFACES

The potential energy surfaces,  $V(\beta, \gamma)$ , for  $^{150}\text{Sm}$  nucleus as a function of the deformation parameters  $\beta$  and  $\gamma$  has been calculated [13] using:

$$\begin{aligned} EN_\nu N_\pi(\beta, \gamma) &= \langle N_\pi N_\nu; \beta\gamma | H_{np} | N_\pi N_\nu; \beta\gamma \rangle = \\ &= \varepsilon_d(N_\nu + N_\pi)\beta^2(1 + \beta^2)^{-1} + \beta^2(1 + \beta^2)^{-2} \cdot \\ &\cdot \left\{ kN_\pi N_\nu \left[ 4 - (\bar{X}_\pi + \bar{X}_\nu)\beta \cos 3\gamma + \bar{X}_\pi \bar{X}_\nu \beta^2 \right] + \right. \\ &\left. + N_\nu(N_\nu - 1) \left( \frac{C_0}{10} + \frac{C_2}{7} \right) \beta^2 \right\} \end{aligned} \quad (9)$$

where

$$\bar{X}_\rho = \sqrt{\frac{2}{7}} X_\rho \quad \rho = \pi \text{ or } \nu \quad (10)$$

The contour plot of the potential energy surfaces are presented in Fig. 1. The three dimensional plot of the potential energy surfaces and deformation parameter  $\beta$  is shown in Fig. 2 at different values of  $\beta$  and  $\gamma$  ( $\gamma$  varied between  $0^\circ$

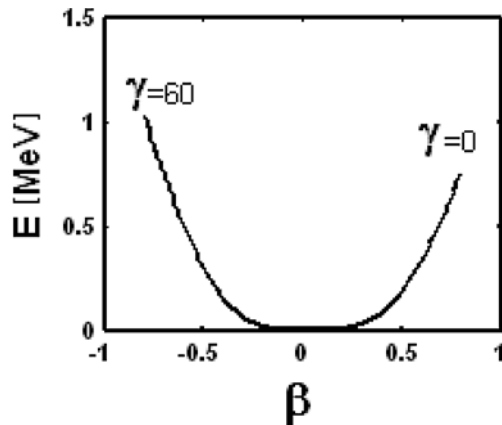


Fig. 1 – Contour plot of the potential energy surfaces.

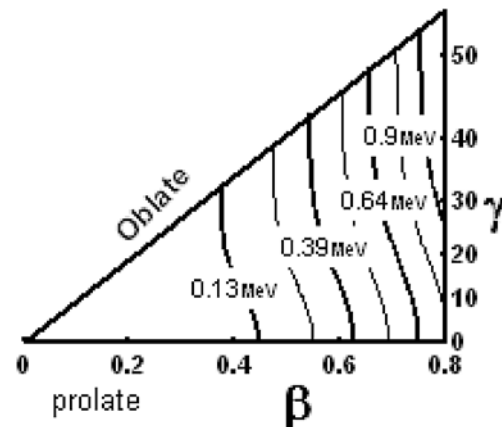


Fig. 2 – The potential deformation energy  $E$  (MeV) versus the deformation  $\beta$  and  $\gamma$ .

and  $60^\circ$ ). It is clear from the graphs that  $^{150}\text{Sm}$  nucleus has vibrational character since vibrational character require:

- (a) minimum surface energy at deformation  $\beta = 0$ ,
- (b) circular contours around  $\beta = 0$ . The two requirements are exist for the nucleus as shown in Figs. 1, 2. The previous arguments support the assumption made by other authors [7, 14] that  $^{150}\text{Sm}$  is a vibrational-like nucleus.

The value of the deformation parameter  $\beta$  which is corresponding to the minimum value of the potential energy implies a decrease of the moment of inertia, and in turn to an increase of the spacing between levels in the ground state and  $\beta$  bands.

### 3.2. LEVEL ENERGIES

The calculated excitation energies of seventeen positive parity levels to  $^{150}\text{Sm}$  are given in Table 1 and displayed in Fig. 3. The agreement between the

Table 1

The positive-parity level energies of  $^{150}\text{Sm}$

band	$I^+$	$E$ (MeV) *Exp.	$E$ (MeV) IBA-2
g.s.b.	0	0.000	0.000
	$2_1$	0.334	0.341
	$4_1$	0.773	0.777
	$6_1$	1.279	1.301
	$8_1$	1.837	1.904
$\beta_1$ b	$0_2$	0.740	0.915
	$2_2$	1.046	0.853
	$4_2$	1.449	1.390
	$6_2$	2.107	1.991
	$8_2$	-----	2.651
$\beta_2$ b	$0_3$	1.256	1.458
	$2_4$	1.417	1.774
	$4_4$	1.672	2.026
$\gamma_1$ b	$2_3$	1.194	1.443
	$3_1$	1.505	1.399
	$4_3$	1.643	2.019
	$0_4$	-----	2.069
	$3_2$	2.063	1.923

\* Ref (17)

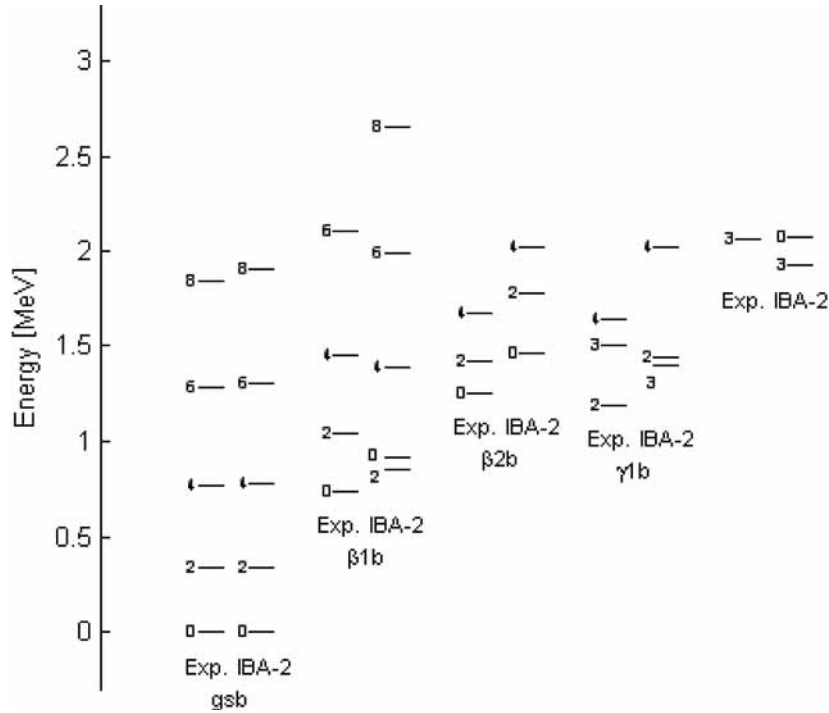


Fig. 3 – Comparison between the experimental and theoretical levels energy in  $^{150}\text{Sm}$ .

calculated and experimental values measured by other authors is satisfactory. Levels are classified into bands according to their energies, transition probability values considering the classifications by other authors [15].

The hamiltonian parameters of eq. (1) used in the present calculation are:

$$\varepsilon = 0.620 \quad K = -0.076 \quad X_{\pi} = -1.300 \quad X_{\nu} = 0.320 \quad \varepsilon_1 = \varepsilon_3 = 0.090$$

$$\varepsilon_2 = 0.100 \quad C_{L\nu} = 0.000, 0.050, 0.000$$

$$C_{L\pi} = 0.000, -0.080, 0.000 \quad \text{all in MeV.}$$

The computer codes NPBOS and NPBEM [16] of the IBA-2 have been used in calculating energy eigenvalues, wave functions and  $E2$  transition matrix elements. It should be noted that in our calculation, we always demand that the energy of the  $2_1^+$  state agrees exactly with experiment, and thus, in this sense we always have a fixed value of the moment of inertia (for any given nucleus). Then, a pushing of the outside potential wall to a smaller value of  $\beta$  means that the nucleus is forced to behave more like a spherical than like a deformed nucleus. The spacing between the higher members of the band in turn being forced to become closer to that between the  $2_1^+$  and  $0_1^+$  states.

3.3. REDUCED TRANSITION PROBABILITIES,  $B(E2)$ 's

The proton and neutron effective charges  $e_\pi$  and  $e_\nu$  were determined using the experimental reduced transition probability [18]  $B(E2, 2_1^+ \rightarrow 0_1^+) = 0.264 \pm \pm 0.012e^2b^2$  with the help of equation [12] for the vibrational limit. The calculated values are:

$$e_\pi = 0.231 \text{ e.b} \quad \text{and} \quad e_\nu = 0.531 \text{ e.b}$$

The transition probabilities of  $B(E2)$ 's are calculated and normalized to the previous experimental value and presented in Table 2. Unfortunately, no more experimental data are available for comparison with the present calculations.

Table 2

Values of the reduced transition probability,  $B(E2)$  (in  $e^2b^2$ ), of  $^{150}\text{Sm}$

$I_i^+$	$I_f^+$	$B(E2)$ Exp*.	$B(E2)$ IBA-2	$I_i^+$	$I_f^+$	$B(E2)$ Exp*.	$B(E2)$ IBA-2
2 <sub>1</sub>	0 <sub>1</sub>	0.264(12)	0.2639	3 <sub>2</sub>	4 <sub>4</sub>		0.0047
2 <sub>1</sub>	0 <sub>2</sub>		0.0342	4 <sub>1</sub>	2 <sub>1</sub>		0.4021
2 <sub>1</sub>	0 <sub>3</sub>		0.0008	4 <sub>1</sub>	2 <sub>2</sub>		0.0025
2 <sub>1</sub>	0 <sub>4</sub>		0.0002	4 <sub>1</sub>	2 <sub>3</sub>		0.0401
2 <sub>2</sub>	0 <sub>1</sub>		0.0093	4 <sub>1</sub>	2 <sub>4</sub>		0.0008
2 <sub>2</sub>	0 <sub>2</sub>		0.0345	4 <sub>2</sub>	2 <sub>1</sub>		0.0051
2 <sub>2</sub>	0 <sub>3</sub>		0.0730	4 <sub>2</sub>	2 <sub>2</sub>		0.2417
2 <sub>2</sub>	0 <sub>4</sub>		0.0003	4 <sub>2</sub>	2 <sub>3</sub>		0.0165
2 <sub>3</sub>	0 <sub>1</sub>		0.0000	4 <sub>2</sub>	2 <sub>4</sub>		0.0012
2 <sub>3</sub>	0 <sub>2</sub>		0.1890	4 <sub>3</sub>	2 <sub>1</sub>		0.0001
2 <sub>3</sub>	0 <sub>3</sub>		0.0001	4 <sub>3</sub>	2 <sub>2</sub>		0.0135
2 <sub>3</sub>	0 <sub>4</sub>		0.0617	4 <sub>3</sub>	2 <sub>3</sub>		0.0526
2 <sub>4</sub>	0 <sub>1</sub>		0.0310	4 <sub>3</sub>	2 <sub>4</sub>		0.0033
2 <sub>4</sub>	0 <sub>2</sub>		0.0027	4 <sub>4</sub>	2 <sub>1</sub>		0.0012
2 <sub>4</sub>	0 <sub>3</sub>		0.0031	4 <sub>4</sub>	2 <sub>2</sub>		0.0041
2 <sub>4</sub>	0 <sub>4</sub>		0.0003	4 <sub>4</sub>	2 <sub>3</sub>		0.2312
2 <sub>1</sub>	2 <sub>2</sub>		0.3311	4 <sub>4</sub>	2 <sub>4</sub>		0.0111
2 <sub>1</sub>	2 <sub>3</sub>		0.0012	4 <sub>1</sub>	4 <sub>2</sub>		0.1935
2 <sub>1</sub>	2 <sub>4</sub>		0.0031	4 <sub>1</sub>	4 <sub>3</sub>		0.0115
2 <sub>2</sub>	2 <sub>3</sub>		0.0420	4 <sub>1</sub>	4 <sub>4</sub>		0.0000
2 <sub>2</sub>	2 <sub>4</sub>		0.0020	4 <sub>2</sub>	4 <sub>3</sub>		0.1290
2 <sub>3</sub>	2 <sub>4</sub>		0.0002	4 <sub>2</sub>	4 <sub>4</sub>		0.1031
3 <sub>1</sub>	2 <sub>1</sub>		0.0194	4 <sub>3</sub>	4 <sub>4</sub>		0.0322

(continues)

Table 2 (continued)

$I_i^+$	$I_f^+$	$B(E2)$ Exp*.	$B(E2)$ IBA-2	$I_i^+$	$I_f^+$	$B(E2)$ Exp*.	$B(E2)$ IBA-2
3 <sub>1</sub>	2 <sub>2</sub>		0.3046	6 <sub>1</sub>	4 <sub>1</sub>		0.4679
3 <sub>1</sub>	2 <sub>3</sub>		0.0445	6 <sub>1</sub>	4 <sub>2</sub>		0.0028
3 <sub>1</sub>	2 <sub>4</sub>		0.0123	6 <sub>1</sub>	4 <sub>3</sub>		0.0146
3 <sub>2</sub>	2 <sub>1</sub>		0.0363	6 <sub>1</sub>	4 <sub>4</sub>		0.0322
3 <sub>2</sub>	2 <sub>3</sub>		0.0003	6 <sub>2</sub>	4 <sub>1</sub>		0.0052
3 <sub>2</sub>	2 <sub>4</sub>		0.2751	6 <sub>2</sub>	4 <sub>2</sub>		0.3291
3 <sub>1</sub>	4 <sub>1</sub>		0.1138	6 <sub>2</sub>	4 <sub>3</sub>		0.0005
3 <sub>1</sub>	4 <sub>2</sub>		0.0527	6 <sub>2</sub>	4 <sub>4</sub>		0.0118
3 <sub>1</sub>	4 <sub>3</sub>		0.2827	8 <sub>1</sub>	6 <sub>1</sub>		0.4902
3 <sub>1</sub>	4 <sub>4</sub>		0.0116	8 <sub>1</sub>	6 <sub>2</sub>		0.0034
3 <sub>2</sub>	4 <sub>1</sub>		0.0000	8 <sub>2</sub>	6 <sub>1</sub>		0.0064
3 <sub>2</sub>	4 <sub>2</sub>		0.0000	8 <sub>2</sub>	6 <sub>2</sub>		0.3461
3 <sub>2</sub>	4 <sub>3</sub>		0.0130				

\* Ref (18)

The calculated transition probability values of (1.991 MeV) 6<sub>2</sub><sup>+</sup> and (2.651 MeV) 8<sub>2</sub><sup>+</sup> confirm that the two levels are members of β<sub>1</sub> band where  $B(E2, 6_2^+ \rightarrow 4_2^+) = 0.3291 > B(E2, 6_2^+ \rightarrow 4_1^+) = 0.0054$  and  $B(E2, 8_2^+ \rightarrow 6_2^+) = 0.3461 > B(E2, 8_2^+ \rightarrow 6_1^+) = 0.0064$ .

The g.s., β<sub>1</sub>, β<sub>2</sub>, γ<sub>1</sub> and γ<sub>2</sub> bands are also confirmed where the transition probability of gamma transitions within the band are much greater than their values between other bands.

The levels energy and transition probability ratios in Table 3 confirm the vibrational character to <sup>150</sup>Sm nucleus.

Table 3

The level energies and transition probability ratios of <sup>150</sup>Sm

Quantity	Exp*.	IBA-2	SU(5)	O(6)	SU(3)
$E_{2_2^+} / E_{2_1^+}$	3.13	2.50	2.00	2.50	3.33
$E_{4_1^+} / E_{2_1^+}$	2.32	2.28	2.00	2.50	3.33
$E_{6_1^+} / E_{2_1^+}$	3.83	3.82	3.00	4.50	7.00
$E_{4_2^+} / E_{2_1^+}$	4.34	4.08	3.00	4.50	7.00
$E_{3_1^+} / E_{2_1^+}$	4.51	4.10	3.00	4.50	7.00

(continues)



Table 3 (continued)

Quantity	Exp*	IBA-2	$SU(5)$	$O(6)$	$SU(3)$
$E8_1^+ / E2_1^+$	5.50	5.58	4.00	7.00	12.00
$E4_3^+ / E2_1^+$	4.92	5.92	4.00	7.00	12.00
$\frac{B(E2, 2_2^+ - 0_1^+)}{B(E2, 2_1^+ - 0_1^+)}$	-----	0.04	0.00	0.00	0.00

\* Ref ( 17)

$SU(5)$  = vibrational limit,

$O(6)$  = gamma unstable limit, and

$SU(3)$  = rotational limit.

### 3.2.3 STRENGTH OF THE ELECTRIC MONOPOLE TRANSITIONS, $X_{iff}(E0/E2)$

The electric monopole transitions,  $E0$ , are normally occur between two states of the same spin and parity by transferring energy and zero unit of angular momentum. It is a pure penetration effect where it caused by the electromagnetic interaction between the nuclear charge and the atomic electron which penetrates the nucleus.

The strength of the electric monopole transition,  $X_{iff}(E0/E2)$ , can be determined by [19]:

$$X_{iff}(E0/E2) = 2.54 \times 10^9 \times A^{4/3} \frac{(E_\gamma \text{ MeV})^5}{\Omega_{K,L}} \alpha(E2) \frac{T_e(E0, I_i - I_f)}{T_e(E2, I_i - I_f)} \quad (11)$$

where

$A$  : mass number,

$I_i$  : spin of the initial state where  $E0$  and  $E2$  transitions are depopulating it,

$I_f$  : spin of the final state of  $E0$  transition,

$I_f$  : spin of the final state of  $E2$  transition,

$E_\gamma$  : gamma ray energy,

$\Omega_{kl}$  : electronic factor for  $K, L$  shells (tabulated [20]),

$\alpha(E2)$  : conversion coefficient of the  $E2$  transition,

$T_e(E0, I_i \rightarrow I_f)$  : absolute transition probability of the  $E0$  transition between  $I_i$  and  $I_f$  states, and

$T_e(E2, I_i \rightarrow I_f)$  : absolute transition probability of the  $E2$  transition between  $I_i$  and  $I_f$  states.

The  $E0$  strength can be considered as the ratio between the reduced transition probability of competing  $E0$  and electric quadrupole,  $E2$ , transitions

de-populating the same level. The calculated values are presented in Table 4 and compared to the measured [21] values. The agreement is good for  $0_2 \rightarrow 0_1 \rightarrow 2_1$ ,  $0_3 \rightarrow 0_2 \rightarrow 2_2$  and not good for  $0_3 \rightarrow 0_1 \rightarrow 2_1$ ,  $0_3 \rightarrow 0_2 \rightarrow 2_1$  transitions. It might be due to the small values of the transition probability of the electric quadrupole transitions. Unfortunately, we don't have any more experimental data for comparison and justifying our calculations.

Table 4

$X_{ifj}(E0/E2)$  ratios for  $E0$  transitions in  $^{150}\text{Sm}$

$I_i^+$	$I_f^+$	$I_{if}^+$	$X_{ifj}(E0/E2)$ Exp*	$X_{ifj}(E0/E2)$ IBA-2
0 <sub>2</sub>	0 <sub>1</sub>	2 <sub>1</sub>	0.018	0.018
0 <sub>3</sub>	0 <sub>2</sub>	2 <sub>3</sub>	-----	0.008
0 <sub>3</sub>	0 <sub>1</sub>	2 <sub>1</sub>	0.22(2)	0.0047
0 <sub>3</sub>	0 <sub>2</sub>	2 <sub>1</sub>	6.40(4)	1.130
0 <sub>3</sub>	0 <sub>2</sub>	2 <sub>2</sub>	0.035(5)	0.030
0 <sub>4</sub>	0 <sub>1</sub>	2 <sub>1</sub>	-----	0.088
0 <sub>4</sub>	0 <sub>2</sub>	2 <sub>4</sub>	-----	0.666
0 <sub>4</sub>	0 <sub>1</sub>	2 <sub>1</sub>	-----	0.088

\* Ref (21)

#### 4. SUMMARY AND CONCLUSION

1. The contour plot of the potential energy surfaces  $V(\beta, \gamma)$  shows that  $^{150}\text{Sm}$  is a spherical nucleus and has a vibrational character.
2. The vibrational limit of the IBA-2 has been used and levels energy of seventeen-levels were calculated.
3. The transition probability of seventy-one gamma transitions were calculated and there is no experimental data for comparison except  $B(E2, 2_1^+ \rightarrow 0_1^+) = 0.264(12)$  where the calculated values are normalized to it.
4. The levels are classified into different bands according to their energies, transition probabilities and with the help of other authors classifications [15].
5. The strength of eight electric monopole ( $E0$ ) transitions has calculated. Four experimental data are available, only two of them are in agreement with the theoretically calculated values.

#### REFERENCES

1. G. Palla, H. V. Geramb, C. Pegel, Nucl. Phys. A403, 134 (1983).
2. P. Talon, N. Alamanos, M. Lamehi-Rachti, C. Levi, L. Coulomb, Nucl. Phys. A359, 493 (1981).

3. G. Palla, C. Pegel, Nucl. Phys. A 321, 317 (1979).
4. Akito Arima Joseph Ginocchio, Nobuaki Yoshida, Nucl. Phys. A384, 112 (1982).
5. M. A. Moinester, J. A. Alster, G. Azuelos, A. E. L. Dieperink, Nucl. Phys. A383, 264 (1982).
6. O. Castanos, P. Federman, A. Frank, S. Pittel, Nucl. Phys. A379, 61 (1982).
7. T. Tamura, K. J. Weeks, T. Kishimoto, Nucl. Phys. A347, 359 (1980).
8. A. Arima, F. Iachello, Ann. phys. 123, 468 (1979).
9. A. Arima, F. Iacello, Ann. phys. 99, 253 (1976).
10. A. Arima, F. Iacello, Ann. phys. 111, 201 (1978).
11. G. Puddu, O. Scholten, Nucl. Phys. A 348, 109 (1980).
12. W. D. Hamilton, P. Irback, J. P. Elliott, Phys. Rev. Lett. 53, 2469 (1984).
13. J. N. Ginocchio, M. W. Kirson, Nucl. Phys. A350, 31 (1980).
14. R. J. Keddy, Y. Yoshizawa, B. Elbek, B. Herskind, M. C. Olesen, Nucl. Phys. A113, 676 (1968).
15. M. Sakai, Atom. Data, Nucl. Data. Tab. 31, 399 (1984).
16. T. Otsuka, Program Package NPBOS K. V. I. Report No. 63 (1979).
17. E. derMateosian, J. K. Tuli, Nucl. Data Sheets 75, 827 (1995).
18. S. Raman, C. W. Nestor, Jr., P. Tikkanen, Atom. Data and Nucl. Data Tab. 78, 1 (2001).
19. J. O. Rasmussen, Nucl. Phys. 19, 85 (1960).
20. A. D. Bell, C. E. Avelo, M. G. Davidson, J. P. Davidson, Can. J. Phys. 48, 2542 (1970).
21. O. Scholten May, *Workshop on interacting boson-boson and boson-fermions systems*, Gull Lake, Michigan 28–30 (1984).